



A Journal of the Gesellschaft Deutscher Chemiker

Angewandte Chemie

GDCh

International Edition

www.angewandte.org

Accepted Article

Title: Simultaneous Detection of Carbon Monoxide and Viscosity Changes in Cells

Authors: Jonathan Robson, Markéta Kubánková, Tamzin Bond, Rian Hendley, Andrew White, Marina Kuimova, and James Wilton-Ely

This manuscript has been accepted after peer review and appears as an Accepted Article online prior to editing, proofing, and formal publication of the final Version of Record (VoR). This work is currently citable by using the Digital Object Identifier (DOI) given below. The VoR will be published online in Early View as soon as possible and may be different to this Accepted Article as a result of editing. Readers should obtain the VoR from the journal website shown below when it is published to ensure accuracy of information. The authors are responsible for the content of this Accepted Article.

To be cited as: *Angew. Chem. Int. Ed.* 10.1002/anie.202008224

Link to VoR: <https://doi.org/10.1002/anie.202008224>

COMMUNICATION

Simultaneous Detection of Carbon Monoxide and Viscosity Changes in Cells

Jonathan A. Robson, Markéta Kubánková, Tamzin Bond, Rian A. Hendley, Andrew J. P. White, Marina K. Kuimova* and James D. E. T. Wilton-Ely*

Department of Chemistry, Molecular Sciences Research Hub, Imperial College London, White City Campus, London W12 0BZ, UK.

Abstract: A new family of robust, non-toxic, water-compatible ruthenium(II) vinyl probes allows the rapid, selective and sensitive detection of endogenous carbon monoxide (CO) in live mammalian cells under normoxic and hypoxic conditions. Uniquely, these probes incorporate a viscosity-sensitive BODIPY fluorophore that allows the measurement of microscopic viscosity in live cells via Fluorescence Lifetime Imaging Microscopy (FLIM) in conjunction with measuring CO. This is the first example of a probe that can simultaneously detect CO alongside small viscosity changes in organelles of live cells.

Carbon monoxide (CO) has long been associated with its toxicity, however, this colourless and odourless gas also plays a key role in cellular messaging.^[1] Its anti-inflammatory, anti-proliferative, anti-apoptotic and anti-coagulative properties are now recognised. Intriguingly, under pathophysiological conditions (e.g., inflammation) CO production in cells increases,^[2] and the real-time monitoring of these changes could potentially provide diagnostic information. Hemoglobin is required as a substrate for CO production *in vivo* and the heme oxygenases (HO-1 and HO-2) play a key role in the generation of this gas in mammals. Emerging evidence suggests that the increased generation of HO-derived CO plays a critical role in the resolution of inflammatory processes and alleviation of cardiovascular disorders,^[3] which has driven interest in CO-releasing molecules (CORMs) for therapy.^[4]

A major obstacle is the lack of effective methods to track CO in biological systems in real time.^[5] Imaging with emissive probes has emerged as one of the most powerful techniques to detect biologically important molecules. However, designing selective CO probes for the cellular environment is challenging, with its wide range of reactive species and variation in pH. He^[6] and Chang^[7] pioneered two very different approaches to the fluorogenic sensing of CO in cells. These studies formed the basis for the majority of subsequent reports that used palladium compounds, which release the fluorophore either through carbonylation or protonolysis.^[8-10] These processes are slow at 37 °C, leading to long response times (commonly >40 min), and use potentially cytotoxic, non-ligated heavy metal salts or require organic co-solvents.^[7-11] There is a pressing need for sensitive, selective, rapid and reliable fluorescent CO probes which overcome the limitations listed above.

Another key parameter of intracellular environments is microscopic viscosity (microviscosity). Abnormalities in viscosity are linked to disease and malfunction^[12] through the disruption of diffusion-controlled cell signalling and transport.^[13] Microscopic viscosity in single live cells changes significantly as a result of production of reactive oxygen species (ROS).^[14] Therefore, microviscosity increases could be correlated to CO production

during inflammation and in cardiovascular disorders, which are both accompanied by oxidative stress. Furthermore, in mitochondria, CO is known to play a role in the modulation of ROS formation. This context led us to design a probe for the simultaneous detection of CO and changes in local viscosity.

Molecular rotors are fluorophores that allow quantitative mapping and real-time monitoring of microviscosity changes within a live cell.^[15-17] The non-radiative decay of a fluorescent excited state of a rotor is influenced by viscosity changes.^[16,17] This sensitivity is due to a conformational change, which occurs after excitation, with a viscosity-dependent rate. Intramolecular rotation is impeded in high viscosity environments, causing higher quantum yields and longer fluorescence lifetimes.^[16,17] Fluorescence Lifetime Imaging Microscopy (FLIM) of molecular rotors allows viscosity mapping by spatially resolving the fluorescence decays of the molecular rotors.^[13,14b,c,17,18] Boron dipyrromethene (BODIPY) rotors have emerged as robust and biocompatible rotors with a wide dynamic range of fluorescence lifetimes, from 100 ps to 6 ns, corresponding to a biologically relevant viscosity range of 1 to 5000 cP (centipoise).^[14b,c,18]

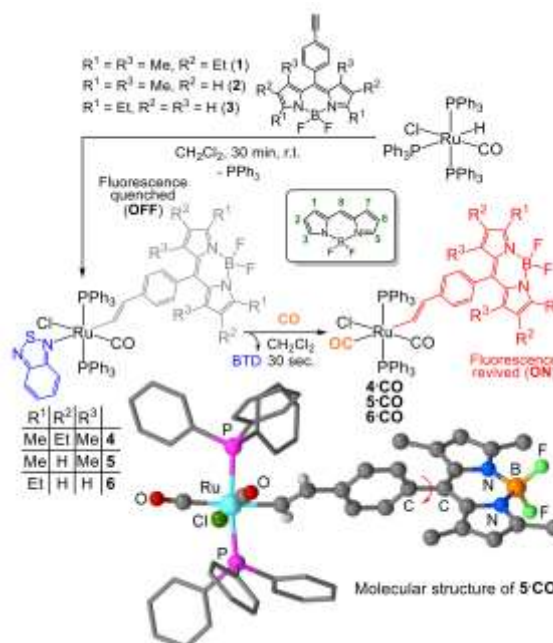


Figure 1. Synthesis of probes 4 – 6 and their reaction with carbon monoxide.

Our previous work on CO detection resulted in a new approach using divalent ruthenium vinyl complexes to deliver combined chromogenic and fluorogenic responses.^[19] Reaction of these compounds with CO results in bright, turn-on emission of a

COMMUNICATION

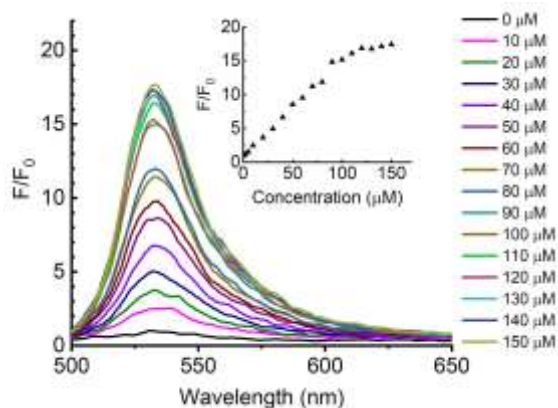


Figure 2. Fluorescence response of **6** (10 μM , pH 7.4, 25 mM PBS–DMSO (9:1 v/v) solution) with 0 - 150 μM CORM-2; $\lambda_{\text{ex}} = 480 \text{ nm}$; insert shows change in fluorescence intensity at 535 nm (ESI, Figure S4-8). F_0 is fluorescence intensity without CO and F is fluorescence intensity upon addition of the CORM-2. PBS = phosphate-buffered saline.

conjugated fluorophore, providing high selectivity and sensitivity towards CO, as demonstrated in an *in vivo* model of inflammation.^[20] The probe design described herein incorporates a BODIPY-based molecular rotor, which not only detects the binding of CO, but also enables the use of FLIM for viscosity monitoring.

Three BODIPY compounds functionalised with a terminal alkyne were prepared (**1** – **3**) and treated with $[\text{RuHCl}(\text{CO})(\text{PPh}_3)_3]$ and 2,1,3-benzothiadiazole (BTD) to yield **4** – **6** (Figure 1) in 72–92% yield (ESI, Section S2). Due to the presence of the BODIPY fluorophore, excitation at 480 nm in dichloromethane led to weak emission ($\Phi_f = 0.009 - 0.10$) at 543 nm. The synthesis routes are summarised in Figure S1-1 (ESI).

The BTD ligand binds *trans* to the vinyl moiety and resists displacement by other species (even high concentrations of MeCN and DMSO).^[19,20] However, on exposure to CO, the BTD ligand is rapidly substituted to yield **4-CO**, **5-CO** (structurally characterised, Figure 1) and **6-CO**, which display significant

fluorescence enhancement (Figures S4-2 to S4-6). The brightest emission ($\Phi_f = 0.77$) was measured for **4-CO**, which displayed a 16-fold revival (Figure S4-3) of the BODIPY fluorescence in pH 7.4, 25 mM PBS–DMSO (9:1 v/v) solution. The instantaneous reaction with CO is a key feature of these probes and a major advantage over Pd-based systems, which require carbonylation or protonolysis to elicit the fluorescence response.^[5,7-10]

Using CORMs to generate CO in aqueous solution (ESI, Section S4),^[21] the performance of the probes was compared (Figures 2 and S4-7). Detection limits were 0.53 μM ($\sim 15 \text{ ppb}$) for **4** and 0.36 μM ($\sim 10 \text{ ppb}$) for **6**. Due to its superior fluorescence enhancement, complex **4** was chosen for sensing CO, while **6** was the only compound sensitive to both CO and viscosity and so was chosen for the combined sensing of both parameters.

The selectivity for CO over other possible interferents was also measured (ESI, Section S6). At pH 7.4, 25 mM PBS–DMSO (9:1 v/v), all compounds were stable (as shown by NMR and fluorescence spectroscopy) towards N_2 , O_2 , CO_2 and exposure to UV light for 24 h. The stability of the probes (10 μM in 1:9 v/v DMSO or acetone:PBS buffer) was investigated with cellular species (bovine serum albumin, aspartic, glutamic, lipoic, citric, folic and ascorbic acids) and ROS (ClO^- , HSO_3^- , SO_3^{2-} , H_2O_2), resulting in negligible changes to the fluorescence of the probes or their CO adducts (ESI, Section S6). The pH of solution has been identified as an issue for stability in recent reports^[5] but negligible fluorescence changes were observed at pH 4 to 10 (ESI, Figure S6-5) for **4** and **6**. Lastly, the probes were found to be non-toxic to MCF-7 cells between 0-200 μM (ESI, Section S7).

To investigate the CO-sensing ability of **4** *in cellulo*, MCF-7 cells were incubated with 10-100 μM CORM-3 and stained with **4**. A clear increase in fluorescence intensity was observed (Figure 3B, Figure S5-4). Probe **4** was also successful in detecting CO generated through the addition of hemin as a substrate for HO-1 catabolism (Figure 3C). Quantification using ImageJ (Figure 3D) revealed a 3-fold increase in fluorescence intensity with CORM-3 and more than a 2-fold increase with hemin.

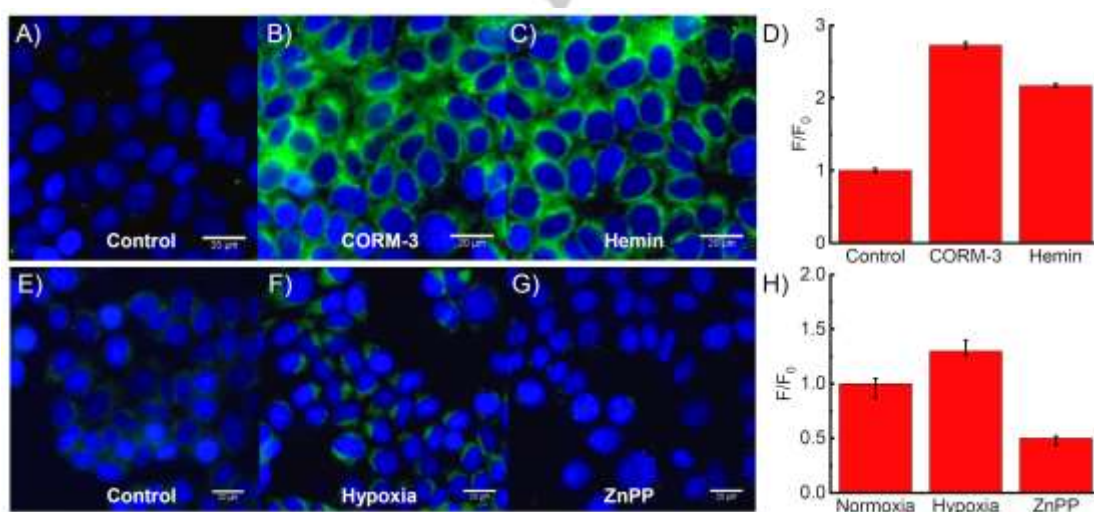


Figure 3. Fluorescence images of **4** (10 μM) (green) and Hoechst 33342 (blue) in MCF-7 cells: A) control - untreated, B) 100 μM CORM-3 for 30 min, C) 100 μM hemin for 5 h, E) Control - pre-incubated in a normoxia incubator (37 $^{\circ}\text{C}$, 5% CO_2 , 95% air) for 24 h, F) pre-incubated in a hypoxia incubator (37 $^{\circ}\text{C}$, 5% CO_2 , 1% O_2 / 99% N_2) for 24 h, G) pre-incubated with Zinc protoporphyrin IX, ZnPP (20 μM) in a hypoxia incubator for 12 h. Integrated change in fluorescence intensity for A, B, C is shown in D and for E, F, G in H (F_0 is fluorescence intensity in control or normoxia and F is fluorescence intensity upon treatment), data expressed as mean \pm SEM of at least three independent experiments. A-D live cells; E-H fixed cells. Scale bars = 20 μm (ESI, Figure S5-5).

COMMUNICATION

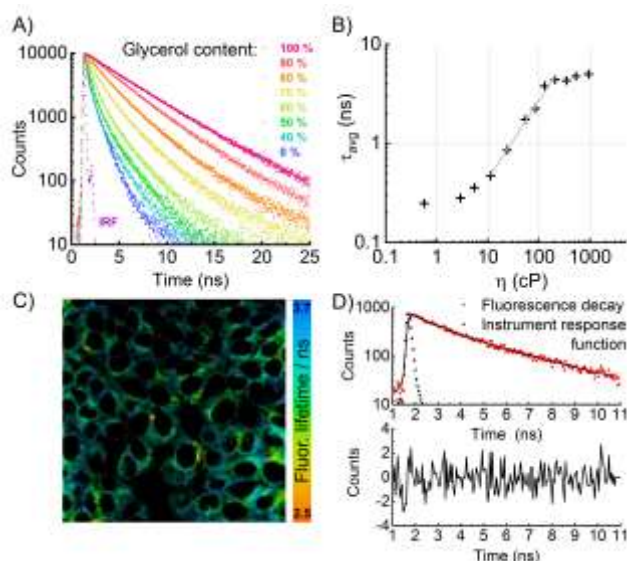


Figure 4. Fluorescence lifetime calibration of probe **6**. A) Time-resolved fluorescence decays recorded in methanol-glycerol mixtures of different viscosities; B) Double-logarithmic calibration plot of average lifetime as a function of viscosity. The linear fit (grey) according to Equation 1 was applicable between 10 and 200 cP; C) FLIM of probe **6** (20 μ M) in live MCF-7 cells. D) Bi-exponential fit of a typical fluorescence decay from a pixel in C) (ESI, Figure S8-7).

Heme oxygenase (HO-1) plays a key role in the generation of cellular CO and is dysregulated in a wide variety of cancers.^[22] Hypoxic conditions can cause an increase in expression of HO-1,^[23] thus probe **4** was tested against CO produced in hypoxia (24 h), in MCF-7 cells, that were treated with **4**, then fixed to maintain the induced effect and compared to cells grown in a normoxia environment. Figure 3F reveals the ability of the probe to detect the resulting endogenous CO. Zinc protoporphyrin IX (ZnPP) inhibits heme oxygenase and thus retards the degradation of heme to CO.^[24] Non-fluorescent ZnPP (ESI, Figure S6-10) was used as an additional control, preventing generation of CO (ESI, Figure S5-2), as evidenced in Figure 3G.

The simultaneous monitoring of carbon monoxide production and viscosity changes was investigated using probe **6**. A key

design element of BODIPY molecular rotors is the viscosity-dependent unrestricted intramolecular twisting at the C8 position (Figure 1)^[13] and **6** is an ideal candidate ($R^3 = H$). Using time-correlated single-photon counting (TCSPC), the time-resolved fluorescence decays of probe **6** were recorded in 0 - 100% glycerol with methanol as a co-solvent. Longer decays were observed as the glycerol percentage increased (Figure 4A), confirming that the probe could successfully detect viscosity changes.

According to the Förster-Hoffmann model,^[25] the plot of $\log \tau$ (fluorescence lifetime, in ps) versus $\log \eta$ (viscosity, in cP) was fitted by a straight line (Figure 4B):

$$\log \tau_{avg} = -10.16 + 0.79 \log \eta \quad (1)$$

Crucially, lifetime-viscosity calibration plots for **6** and **6-CO** (obtained by treating **6** with CO) were almost identical (Figure S8-1), allowing viscosity measurements to be made independent of the presence of CO, while the higher fluorescence intensity of **6-CO** aids signal acquisition. Probe **6** was incubated in cells and FLIM was used to analyse the results (Figure 4C-D), allowing straightforward spatio-temporal detection of the fluorescence lifetime, which correlates with viscosity according to Equation 1.

To test the simultaneous detection of CO and viscosity using **6**, MCF-7 cells were incubated with CORM-2 (0 – 200 μ M) or hemin (0 – 100 μ M). In both cases probe **6** exhibited a clear increase in fluorescence intensity (Figure 5A-E), reporting generation of CO. At the same time, fluorescence decays were recorded to analyse microviscosity. No notable change in average lifetime was observed upon incubation with CORM-2 (Figure 5G,J). Using the fluorescence lifetime-viscosity calibration of **6-CO**, the average lifetime of 3.3 ns corresponded to a viscosity of 133 cP, a typical value for lipid-based intracellular organelles.^[13,14b,c,18]

Intriguingly, the shorter fluorescence lifetime observed upon incubation with hemin (Figure 5I,J) suggested a decrease of intracellular viscosity (to 100 cP, 2.7 ns), which indicates that hemin and CORM-2 treatments (both commonly used to generate CO in cells) do not result in the same cellular environment.

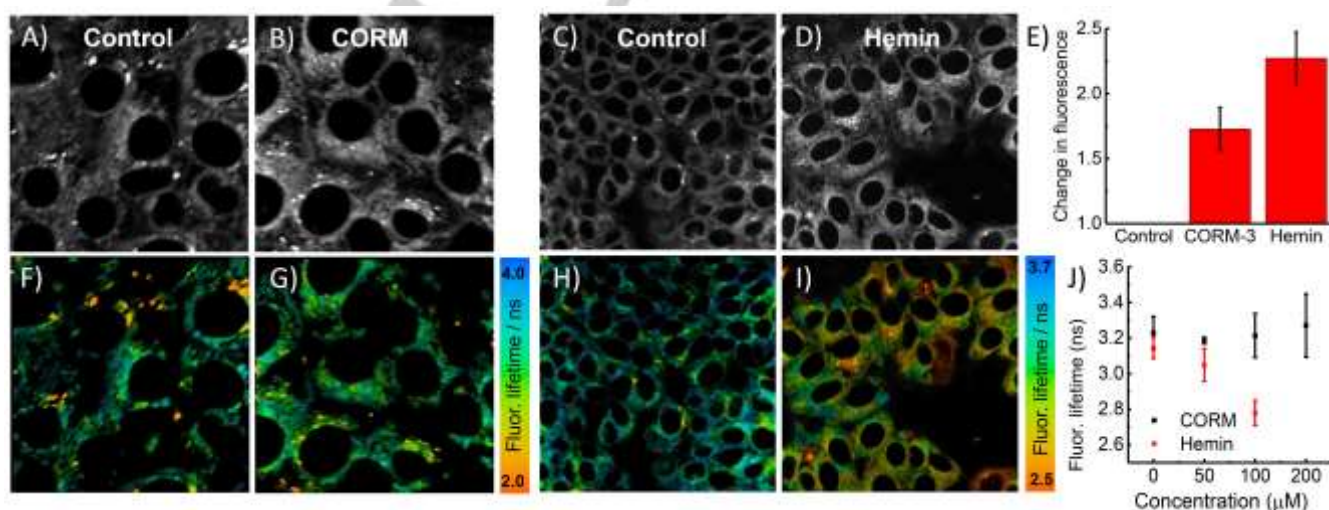


Figure 5. Fluorescence lifetime imaging of **6** (20 μ M) in live MCF-7 cells showing intensity (A-E) and lifetime (F-J); A) and C) controls; B) incubated with 100 μ M CORM-2; D) incubated with 100 μ M hemin. E) Change in fluorescence intensity of cells with CORM-2 and hemin compared to controls. Underneath are the corresponding FLIM images; Data expressed as mean \pm SEM of at least three independent experiments, and at least four FLIM images (ESI, Figure S8-8).

COMMUNICATION

While CORM-2 delivers CO into the cell and produces no changes in viscosity, hemin increases HO-1 expression, modulating ROS inside the cell^[26] and our data reveals that it decreases viscosity. Furthermore, short-lived ROS species may diffuse more easily through the cell due to the lower microviscosity induced by hemin.

Together with the fluorescence intensity data, these results represent the first simultaneous measurement of CO concentration and viscosity in cells. It is also the first example in which molecular rotor is directly linked to a metal-based chemosensor, while preserving its sensitivity to the viscosity of its environment, enabling dual viscosity and CO detection.

Many palladium-based probes have been reported with greater sensitivity for CO than the ruthenium-based system reported here.^[8,10] However, concerns remain over the toxicity of Pd(II) salts^[11] in living systems and the slow response time caused by the need for diffusion controlled co-location of three reaction partners (Pd salt, fluorophore and CO) for detection to occur. Our probe is the only competitive metal-based system not based on palladium and successfully addresses both of these issues. It shows no cytotoxicity even up to 200 μM and instantaneous response to CO through its direct coordination to the metal. Such attributes make these systems highly effective, all-round sensors for the detection of CO in the challenging environment of the cell. This is exemplified by the fact that probe **4** is able to detect endogenous CO generated through increased HO-1 expression under hypoxic conditions. Most significantly, this design represents the first example of a dual modality CO and viscosity probe (**6**), allowing simultaneous measurement of CO through fluorescence intensity and viscosity through fluorescence lifetime. Our experiments show that an increase in HO-1 expression leads to a decrease in cellular viscosity and this result may help to elucidate how HO-1 modulates the activity of radical oxygen species. Our proof-of-concept biological studies provide an insight into the potential of these probes to characterise the mechanisms of delivery and signalling ability of CO within the body.

Acknowledgements

The EPSRC is gratefully acknowledged for studentships to J.A.R. and T.B., and to R.H. as part of the CDT in Smart Medical Imaging (EP/L015226/1). M.K. was supported by an EPSRC Doctoral Prize Fellowship. M.K.K. is grateful to the EPSRC for a Career Acceleration Fellowship (EP/I003983/1). Prof. R. Martínez-Mañez and Dr F. Sancenón are thanked for their contributions and support.

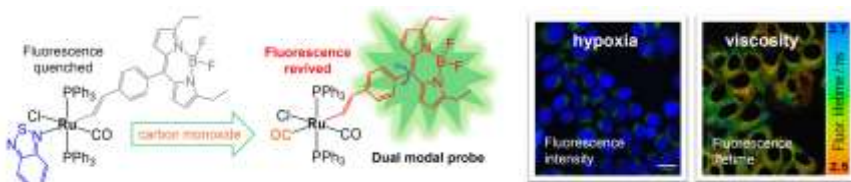
Keywords: Ruthenium, sensing, viscosity, carbon monoxide, fluorescence

- [1] a) T. Sjöstrand, *Nature* **1949**, *164*, 580–581. b) C. Szabo, *Nat. Rev. Drug Discovery* **2016**, *15*, 185–203. c) S. H. Heinemann, T. Hoshi,

- M. Westerhausen, A. Schiller, *Chem. Commun.* **2014**, *50*, 3644–3660.
 [2] L. Wu, R. Wang, *Pharmacol. Rev.* **2005**, *57*, 585–630.
 [3] R. Motterlini, L. E. Otterbein, *Nat. Rev. Drug Discov.* **2010**, *9*, 728–743.
 [4] A. C. Kautz, P. C. Kunz, J. Janiak, *Dalton Trans.* **2016**, *45*, 18045–18063.
 [5] C. Marín-Hernández, A. Toscani, F. Sancenón, J. D. E. T. Wilton-Ely, R. Martínez-Mañez, *Chem. Commun.* **2016**, *52*, 5902–5911.
 [6] J. Wang, J. Karpus, B. S. Zhao, Z. Luo, P. R. Chen, C. A. He, *Angew. Chem. Int. Ed.* **2012**, *51*, 9652–9656; *Angew. Chem.* **2012**, *124*, 9790–9794.
 [7] B. W. Michel, A. R. Lippert, C. J. A. Chang, *J. Am. Chem. Soc.* **2012**, *134*, 15668–15671.
 [8] S. Pal, M. Mukherjee, B. Sen, S. K. Mandal, S. Lohar, P. Chattopadhyay, K. Dhara, *Chem. Commun.* **2015**, *51*, 4410–4413.
 [9] a) K. Zheng, W. Lin, L. Tan, H. Chen, H. Cui, *Chem. Sci.* **2014**, *5*, 3439–3448. b) K. Liu, X. Kong, Y. Ma, W. Lin, *Angew. Chem. Int. Ed.* **2017**, *56*, 13489–13492; *Angew. Chem.* **2017**, *129*, 13674–13677.
 [10] E. Zhou, S. Gong, G. Feng, *Sens. Act. B* **2019**, *301*, 127075.
 [11] C. Zhang, H. Xie, T. Zhan, J. Zhang, B. Chen, Z. Qian, G. Zhang, W. Zhang, J. Zhou, *Chem. Commun.* **2019**, *55*, 9444–9447
 [12] K. Luby-Phelps, *Int. Rev. Cytol.* **2000**, *192*, 189–221.
 [13] M. K. Kuimova, G. Yahioglu, J. A. Levitt, K. Suhling, *J. Am. Chem. Soc.* **2008**, *130*, 6672–6673.
 [14] a) M. K. Kuimova, S. W. Botchway, A. W. Parker, M. Balaz, H. A. Collins, H. L. Anderson, K. Suhling, P. R. Ogilby, *Nature Chem.* **2009**, *1*, 69–73. b) M. Kubánková, I. López-Duarte, D. Kiryushko, M. K. Kuimova, *Soft Matter*, **2018**, *14*, 9466–9474. c) M. Kubánková, P. A. Summers, I. López-Duarte, D. Kiryushko, M. K. Kuimova, *ACS Appl. Mater. Interfaces* **2019**, *11*, 36307–36315.
 [15] Z. Yang, J. Cao, Y. He, J. H. Yang, T. Kim, X. Peng, J. S. Kim, *Chem. Soc. Rev.* **2014**, *43*, 4563–4601.
 [16] M. A. Haidekker, E. A. Theodorakis, *Org. Biomol. Chem.* **2007**, *5*, 1669–1678.
 [17] M. K. Kuimova, *Phys. Chem. Chem. Phys.* **2012**, *14*, 12671–12686.
 [18] J. E. Chambers, M. Kubánková, R. G. Huber, I. López-Duarte, E. Avezov, P. J. Bond, S. J. Marciniak, M. K. Kuimova, *ACS Nano* **2018**, *12*, 4398–4407.
 [19] a) M. E. Moragues, A. Toscani, F. Sancenón, R. Martínez-Mañez, A. J. P. White, J. D. E. T. Wilton-Ely, *J. Am. Chem. Soc.* **2014**, *136*, 11930–11933. b) A. Toscani, C. Marín-Hernández, M. E. Moragues, F. Sancenón, F. Dingwall, N. J. Brown, R. Martínez-Mañez, A. J. White, J. D. E. T. Wilton-Ely, *Chem. Eur. J.* **2015**, *21*, 14529–14538. c) A. Toscani, C. Marín-Hernández, J. A. Robson, E. Chua, P. Dingwall, A. J. P. White, F. Sancenón, C. de la Torre, R. Martínez-Mañez, J. D. E. T. Wilton-Ely, *Chem. Eur. J.* **2019**, *25*, 2069–2081.
 [20] C. de la Torre, A. Toscani, C. Marín-Hernández, J. A. Robson, M. C. Terencio, A. J. P. White, M. J. Alcaraz, J. D. E. T. Wilton-Ely, R. Martínez-Mañez, F. Sancenón, *J. Am. Chem. Soc.* **2017**, *139*, 18484–18487.
 [21] M. Klein, U. Neugebauer, A. Gheisari, A. Malassa, T. M. A. Jazzazi, F. Froehlich, M. Westerhausen, M. Schmitt, J. Popp, *J. Phys. Chem. A* **2014**, *118*, 5381–5390.
 [22] P. Podkalicka, O. Mucha, A. Józkwicz, J. Dulak, A. Łoboda, *Contemp. Oncol. (Pozn)*. **2018**, *22*, 23–32.
 [23] T. Morita, M. A. Perrella, M. E. Lee, S. Kourembanas, *PNAS* **1995**, *92*, 1475–1479.
 [24] C. Zhou, J. Zhou, F. Sheng, H. Zhu, X. Deng, B. Xia, J. Lin, *Acta Biochim. Biophys. Sin.* **2012**, *44*, 815–822.
 [25] T. Förster, G. Hoffmann, *Z. Phys. Chem.* **1971**, *75*, 63–76.
 [26] J. Araujo, M. Zhang, F. Yin, *Front. Pharmacol.* **2012**, *3*, 119.

COMMUNICATION

Entry for the Table of Contents



Carbon monoxide (CO) is produced in mammals and regulates many critical cellular functions, including the response to disease. This work reports a ruthenium(II) vinyl probe that allows the rapid, selective and sensitive detection of endogenous CO in live mammalian cells under normoxic and hypoxic conditions. By exploiting Fluorescence Lifetime Imaging Microscopy, the probe can also measure microscopic viscosity in live cells at the same time.

Institute and/or researcher Twitter usernames: @JWElab